International Journal of Medical Toxicology & Forensic Medicine
2026, Volume 16, E53560

Research Paper

Multiorgan Caspase-3 Immunoreactivity and Physiopathological Injury Following Chronic Oral Aluminum Chloride Exposure in Rats

Hawraa M. Murad[1*], Ahmed Neema AL-Mussawy[2], Ghusoon Abdul Kareem Neamah[3], Shurooq Asaad Abdulameer Shaher[4]

1. *Department of Biology, College of Science, Al-Qasim Green University, Babylon 51013, Iraq.*
2. *Department of Biology, College of Science, University of Kerbala, Kerbala, Iraq.*
3. *Department of Pathology and Poultry Diseases, College of Veterinary Medicine, Al-Qasim Green University, Babylon 51013, Iraq.*
4. *Department of Radiology and Ultrasound, Babylon College of Health and Medical Technology, Al-Furat Al-Awsat Technical University, Babylon, Iraq.*

Citation Murad HM, AL-Mussawy AN, Neamah GAK, Shaher SAA. Multiorgan Caspase-3 Immunoreactivity and Histopathological Injury Following Chronic Oral Aluminum Chloride Exposure in Rats. International Journal of Medical Toxicology and Forensic Medicine. 2026; 16:E53560.

https://doi.org/10.22037/ijmtfm.v16.53560

Article info:

Received: 23 September, 2026

Accepted: 18 October, 2026

Published: 30 October, 2026

Keywords:

Aluminum Chloride, Caspase 3, Histopathology, Immunohistochemistry, Rats

ABSTRACT

Background: Aluminum exposure can injure multiple organs, but its association with tissue-specific caspase-3 immunoreactivity remains incompletely characterized.

Methods: Ninety male rats, aged 8–9 weeks and weighing 200–300 g, received distilled water or aluminum chloride hexahydrate (100 or 200 mg/kg/day) by oral gavage. We sampled ten rats per group on days 30, 60, and 90. We assessed serum calcium and iron and evaluated tissue histopathology. We quantified caspase-3-positive cells in four organs of control and high-dose rats at day 90.

Results: At day 90, high-dose rats had lower calcium (5.43±0.24 versus 10.55±0.23 mg/dL) and iron (5.56±0.08 versus 11.33±0.17 µmol/L) than controls. Approximate mean differences were −5.12 mg/dL (95% CI, −5.56 to −4.68) and −5.77 µmol/L (−6.22 to −5.32), respectively. Caspase-3-positive counts increased in all four organs (Holm-adjusted $p<0.001$). Histology showed renal tubular degeneration, hepatic vacuolation, and splenic lymphoid depletion, congestion, hemosiderosis, and follicular apoptotic bodies.

Conclusion: Chronic oral aluminum chloride exposure was associated with increased caspase-3 immunoreactivity, renal, hepatic, and splenic histopathological injury, and reduced serum calcium and iron. The immunostaining indicates caspase-3 protein immunoreactivity, not confirmed enzymatic activation or apoptosis; the data do not establish an organ-susceptibility ranking.

*** Corresponding Author:**
Hawraa M. Murad, PhD
Department of Biology, College of Science, Al-Qasim Green University, Babylon 51013, Iraq.
E-mail: *hawraa@vet.uoqasim.edu.iq*

Copyright © 2026 The Author(s);
This is an open-access article distributed under the terms of the Creative Commons Attribution-NonCommercial 4.0 International License (CC BY-NC 4.0: https://creativecommons.org/licenses/by-nc/4.0/), which permits unrestricted non-commercial use, distribution, and reproduction in any medium, provided the original work is properly cited.

Introduction

Aluminum is a ubiquitous, non-essential metal used in packaging, water treatment, pharmaceuticals, and industrial processes. Although gastrointestinal absorption is limited, sustained exposure can result in accumulation and neurological, renal, hepatic, hematological, and skeletal abnormalities [1, 2].

Oxidative and mitochondrial disturbances have been proposed in experimental aluminum-associated liver injury [3]. Aluminum also alters iron-binding systems [4], intestinal calcium transport [5], and calcium-regulatory processes [2]. Calcium signaling participates in mitochondrial regulation and cell-death pathways [6], providing a biological context for examining circulating minerals alongside structural injury.

Apoptotic pathways converge on effector caspases [7]. Caspase-3 becomes active after proteolytic processing [8]; a non-cleavage-specific antibody detects protein immunoreactivity rather than activation. Aluminum-associated caspase changes have been reported in rat splenic lymphocytes, hippocampus, liver, and kidney [9–11], but tissue staining cannot be assumed directly comparable across organs.

Previous studies reported brain aluminum accumulation, oxidative-stress markers, acetylcholinesterase activity, and neural histopathology from the same experimental cohort [12]. The present study examines distinct endpoints: serum calcium and iron concentrations, caspase-3 immunoreactivity in neural and peripheral tissues, and renal, hepatic, and splenic histopathology. Its objective was to characterize these biochemical and morphological findings during chronic oral aluminum chloride exposure, with quantitative immunohistochemical comparisons restricted to four organs in control and high-dose animals at day 90.

Materials and Methods

Ethical approval and reporting

The Institutional Animal Care and Use Committee, College of Veterinary Medicine, Al-Qasim Green University, Babylon, Iraq, approved the procedures (QGEC/3/2025). Care followed national requirements and the principles of replacement, reduction, and refinement. Reporting followed the ARRIVE 2.0 Essential 10 [13].

Animals, housing, and experimental design

Ninety male albino rats (Rattus norvegicus), aged 8–9 weeks and weighing 200–300 g at study entry, were obtained from the National Center for Drug Control and Research, Baghdad, Iraq. After 14-day acclimatization, we housed five rats per polypropylene cage at 22±2 °C and 50±10% humidity under a 12-hour light/dark cycle, with a commercial pelleted diet and tap water ad libitum. We observed animals twice daily and weighed them weekly.

Computer-generated random numbers allocated 30 rats each to distilled-water control or aluminum chloride hexahydrate at 100 or 200 mg/kg/day by daily oral gavage for up to 90 days. Cage position was randomized. We assigned 10 rats per group before dosing to terminal sampling on days 30, 60, or 90. Dose selection referenced previous rodent research [14]; successive time points involved different animals.

The cohort also supported the previous neural study [12]. We do not reproduce or reanalyze its numerical data or images here; the present serum, immunohistochemical, and peripheral histopathological endpoints are distinct.

Inclusion and exclusion criteria

The study included male rats within the stated baseline age and weight ranges. All 90 randomized animals were analyzed; none was excluded.

Sample collection

At each terminal time, rats were fasted overnight and anesthetized intraperitoneally with ketamine (90 mg/kg) and xylazine (10 mg/kg). We collected approximately 5 mL of blood by cardiac puncture, allowed it to clot in anticoagulant-free tubes for 30 minutes at room temperature, and centrifuged it at 3000 rpm (approximately 1000×g) for 5 minutes. Serum was stored at −20°C without repeated freeze–thaw cycles. Cervical dislocation was performed under anesthesia; absent corneal reflex and cardiac activity confirmed death.

Serum calcium and iron assays

We measured serum calcium and iron in duplicate using research-use-only microplate assay kits (MyBioSource Inc., San Diego, CA, USA; reported catalog nos. MBS6048568 and MBS3808464, respectively) according to the instructions supplied with the kits. We read absorbance at 450 nm and calculated concentrations from plate-specific standard curves. We distributed samples from all time points across plates. Reported intra-assay and inter-assay coefficients of variation were <8% and <10%, respectively. Calcium is reported in mg/dL. Iron is reported in µmol/L, consistent with the standard concentrations specified in the manufacturer's protocol

for MBS3808464. Duplicate wells were technical replicates, not independent experimental units.

Histopathology

We fixed cerebrum, cerebellum, kidney, liver, and spleen specimens in 10% neutral-buffered formalin for 48 hours, processed them routinely, embedded them in paraffin, sectioned them at 5 µm, and stained them ppll;with hematoxylin and eosin [15]. Sections were examined at ×100 and ×400 by two pathologists blinded to group assignment. We described renal tubular degeneration and interstitial congestion, hepatic vacuolation and centrilobular congestion, and splenic lymphoid depletion, red-pulp congestion with hemosiderosis, and follicular apoptotic bodies. We reported the histopathological assessment qualitatively and did not use it to estimate animal-level lesion frequencies or compare ordinal severity distributions. Neural hematoxylin–eosin findings from this cohort were reported previously [12] and are not presented again.

Caspase-3 immunohistochemistry and quantification

Four-micrometer sections on positively charged slides were deparaffinized, rehydrated, and retrieved in 10 mM citrate (pH 6.0; 95°C, 30 minutes). Peroxidase/protein blocking lasted 20 minutes/1 hour. Rabbit polyclonal anti-caspase-3 (E-AB-63510; Elabscience, Houston, TX, USA; 1:4000) was applied for 2 hours at 37 °C. PolyExcel Target Binder/PolyHRP and diaminobenzidine detected the signal, followed by Mayer hematoxylin. Rat intestinal mucosa was the positive control; primary-antibody omission provided negative controls.

Two blinded observers counted brown cytoplasmic/nuclear-positive cells among 1000 cells across at least 10 random, non-overlapping ×400 fields per rat/organ. Their counts were averaged per rat (n=10/group). Rats, not fields, cells, observers, or duplicate wells, were the independent experimental units. The antibody was not cleavage-specific; staining represents caspase-3 protein immunoreactivity.

Quantification comprised cerebrum, kidney, liver, and spleen from control and 200 mg/kg/day rats at day 90. Counts were unavailable for other dose/time combinations or cerebellum. Cerebellar panels illustrate localization only; no full immunohistochemical dose–time response was tested.

Statistical analysis

We used SPSS Statistics 20 (IBM, Armonk, NY, USA), with Shapiro–Wilk and Levene tests. Serum outcomes used two-way ANOVA with group (three levels), terminal sampling time (three levels), and interaction; immunohistochemical counts used organ-specific two-group one-way ANOVA. Serum values are mean±SE, and cell counts mean±SD.

Reported means, dispersion, and n=10 permitted algebraic ANOVA and confidence-interval calculations. For serum, within-cell variance was $n\times SE^2$ and residual sums of squares $\Sigma(n-1)n\times SE^2$. Group/time/interaction numerator degrees of freedom were 2/2/4, with 81 residual degrees of freedom; serum contrasts used the model residual variance and t(81). Immunohistochemical comparisons used pooled variance and 18 residual degrees of freedom. Estimates derived from rounded summaries are approximate; confidence intervals are pointwise, not simultaneous.

Least significant difference contrast p-values were Holm-adjusted [16] within separate families of 18 comparisons per analyte: nine between-group and nine between-time contrasts. Four organ-specific comparisons formed another family. Tests were two-sided ($\alpha=0.05$). Key numerical statistics and confidence intervals are reported in the Results and Table 1.

Results

Clinical observations

No deaths occurred. All 90 animals were retained, with 10 per group at each sampling time.

Caspase-3 immunor0eactivity

Day-90 caspase-3-positive counts were higher in high-dose animals than controls within each quantified organ (all Holm-adjusted $p<0.001$; Table 1). No cross-organ susceptibility ranking was tested.

Staining involved cerebral neurons/neuropil, cerebellar granular and Purkinje-cell regions, renal tubular epithelium, splenic white-pulp/periarteriolar regions, and predominantly periportal hepatic tissue (Figure 1). Controls showed less staining, although renal immunoreactivity was evident. Cerebellar observations were qualitative.

Renal, hepatic, and splenic histopathology

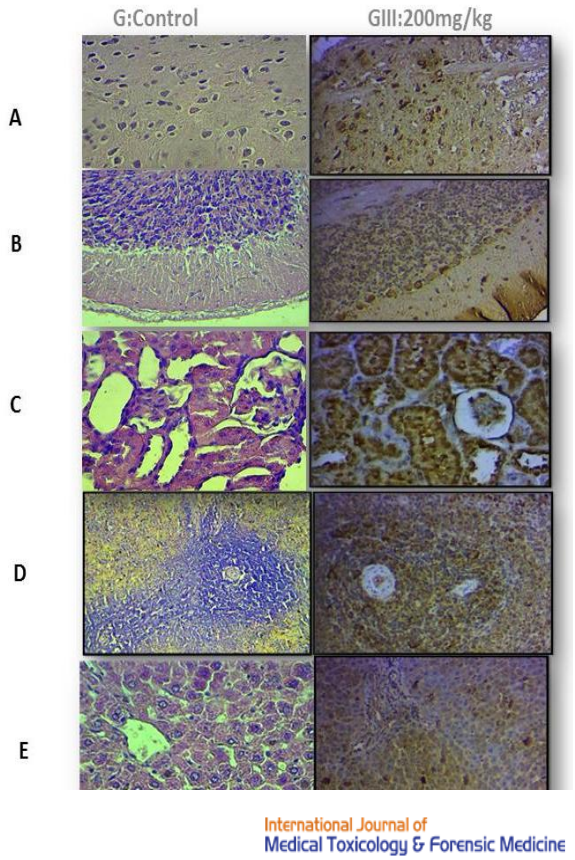
Table 2 summarizes the observed abnormalities. Day-90 high-dose spleens showed white-pulp depletion, red-pulp congestion with hemosiderosis, and follicular apoptotic bodies. Kidneys showed tubular degeneration, vacuolation, sloughing, and interstitial congestion, with relatively preserved glomeruli. The

Table 1. Day-90 caspase-3-positive cell counts and within-organ differences.

Organ	Control (mean±SD)	200 mg/kg/day (mean±SD)	Difference (pointwise 95% CI)	Holm-adjusted p (approximate)
Cerebrum	4.00±0.58	80.33±6.23	76.33 (72.17 to 80.49)	1.85×10^{-18}
Kidney	33.00±0.85	66.67±1.20	33.67 (32.69 to 34.65)	3.58×10^{-23}
Liver	7.67±0.33	26.00±3.51	18.33 (15.99 to 20.67)	2.75×10^{-12}
Spleen	4.67±0.33	45.00±0.58	40.33 (39.89 to 40.77)	1.27×10^{-30}

International Journal of Medical Toxicology & Forensic Medicine

Positive cells per 1000 counted cells; n=10 independent rats/group. Differences are high-dose minus control. Estimates use rounded means/SD and the two-group ANOVA model (residual df=18); p values are Holm-adjusted across four organs.



International Journal of Medical Toxicology & Forensic Medicine

Figure 1. Caspase-3 immunohistochemistry in controls (left) and rats receiving 200 mg/kg/day aluminum chloride for 90 days (right): (A) cerebrum, neurons/neuropil; (B) cerebellum, granular/Purkinje-cell regions; (C) kidney, tubular epithelium; (D) spleen, white-pulp/periarteriolar regions; (E) liver, hepatocytes/periportal tissue. Brown diaminobenzidine indicates protein immunoreactivity; Mayer hematoxylin counterstain, original magnification ×400. Cerebellar panels were not quantified.

liver showed centrilobular congestion, hydropic vacuolation, and occasional pyknotic nuclei. Control architecture remained normal at sampled times. These observations were qualitative.

Serum calcium and iron

Calcium declined with dose and sampling time in treated rats; control means were similar (Table 3). Day-90 high-dose–control difference was approximately −5.12 mg/dL (95% CI, −5.56 to −4.68; Holm-adjusted $p\approx2.77\times10^{-36}$), a 48.5% lower mean. Between-group comparisons at every time remained significant after adjustment.

Table 2. Qualitative renal, hepatic, and splenic histopathological observations.

Tissue	Observations in aluminum-exposed animals	Reported control architecture
Kidney	Tubular epithelial degeneration and vacuolation; epithelial sloughing; interstitial congestion; relative preservation of glomeruli.	Normal architecture at the sampled time points.
Liver	Centrilobular congestion; hydropic hepatocellular vacuolation; occasional pyknotic nuclei.	Normal architecture at the sampled time points.
Spleen	White-pulp lymphoid depletion; red-pulp congestion with hemosiderosis; follicular apoptotic bodies. These observations were described in day-90 high-dose animals.	Normal architecture at the sampled time points.

International Journal of Medical Toxicology & Forensic Medicine

Qualitative observations only; animal-level lesion incidence, grade frequencies, and ordinal dose–time progression were not estimated.

Iron was lower in exposed groups (Table 3). High-dose values decreased successively, reaching 5.56±0.08 versus 11.33±0.17 µmol/L in controls at day 90: approximate difference −5.77 µmol/L (95% CI, −6.22 to −5.32; adjusted $p\approx5.60\times10^{-39}$), a 50.9% lower mean. Low-dose day-90–day-60 difference was nonsignificant (0.29 µmol/L; 95% CI, −0.16 to 0.74; adjusted p≈0.827).

Summary-based calcium ANOVA terms were group $F(2,81)=588.95$ ($p\approx5.54\times10^{-49}$), time $F(2,81)=38.21$ ($p\approx2.06\times10^{-12}$), and interaction

Table 3. Serum calcium and iron concentrations during aluminum chloride exposure.

Analyte	Group	Day 30	Day 60	Day 90
Calcium (mg/dL)	Control	10.50±0.23	10.53±0.23	10.55±0.23
	100 mg/kg/day	9.83±0.03	9.16±0.03	8.13±0.02
	200 mg/kg/day	7.12±0.01	6.12±0.02	5.43±0.24
Iron (µmol/L)	Control	11.37±0.17	11.35±0.17	11.33±0.17
	100 mg/kg/day	9.56±0.24	8.14±0.01	8.43±0.26
	200 mg/kg/day	7.16±0.03	6.30±0.12	5.56±0.08

International Journal of
Medical Toxicology & Forensic Medicine

Mean±SE; n=10 independent rats/group/time. Calcium is in mg/dL and iron in µmol/L. Key contrasts and approximate ANOVA terms are reported in Section 3.4. SE, standard error.

$F(4,81)=10.81$ ($p\approx4.50\times10^{-7}$). Corresponding iron terms were $F(2,81)=725.67$ ($p\approx1.94\times10^{-52}$), $F(2,81)=28.21$ ($p\approx5.05\times10^{-10}$), and $F(4,81)=9.09$ ($p\approx4.07\times10^{-6}$), respectively. Interactions indicate that time differences depended on exposure group.

Discussion

Chronic oral aluminum chloride exposure in this study was associated with increased caspase-3 immunoreactivity in the cerebrum, kidney, liver, and spleen, together with renal, hepatic, and splenic histopathological abnormalities and lower serum calcium and iron. The quantitative immunohistochemical findings represent within-organ differences between high-dose and control animals at day 90. They do not establish a hierarchy of organ susceptibility because baseline expression, cellular composition, and tissue architecture differ among organs. Similarly, the non-cleavage-specific antibody identifies caspase-3 protein immunoreactivity, not enzymatic activation. The observed staining and lesions therefore support aluminum-associated tissue injury but do not independently confirm the underlying cell-death pathway.

The neural staining pattern extends the anatomical observations from the earlier report of oxidative and histopathological findings in this cohort [12], without reproducing those endpoints. In a separate 90-day oral rat model, Zhang et al. reported increased hippocampal caspase-3 activity and expression, an increased Bax/Bcl-2 mRNA ratio, and greater TUNEL positivity alongside IL-1β/JNK activation [10]. Their complementary endpoints provide mechanistic context for the present cerebral staining, but their hippocampal measurements do not match the whole-cerebrum immunohistochemical assessment used here. Mesole et al. also reported increased brain caspase-3 activity and apoptosis-associated biochemical changes after 21 days of oral aluminum chloride exposure, with attenuation by eugenol [17]. Differences in brain region, exposure duration, and assay design preclude direct quantitative comparison. Cerebellar staining in the present study remains a qualitative localization finding, rather than evidence of a separately quantified cerebellar response.

Splenic immunoreactivity accompanied lymphoid depletion, congestion, hemosiderosis, and follicular apoptotic bodies. Li et al. reported mitochondrial caspase-associated apoptosis in rat splenic lymphocytes [9]; Khalaf et al. described altered immune responses after prenatal/postnatal exposure [18]. Yu et al. observed melatonin attenuating splenic oxidative and apoptosis-associated changes in a 90-day rat model [19]. These studies contextualize the lesions, but the present morphology and immunostaining do not establish functional immunosuppression or caspase-3 activation.

Renal tubular staining corresponded anatomically with degeneration and sloughing. Liu et al. linked aluminum-associated renal injury to mitochondrial damage and protective PINK1/Parkin quality control in a mouse drinking-water model [20]. Wei et al. implicated TGF-β1/Smads signaling in renal apoptosis/fibrosis after four-week intraperitoneal rat exposure and in HK-2 cells [21]. Hepatic vacuolation and congestion are also consistent with proposed oxidative injury [3] and Othman et al.'s hepatorenal antioxidant/histological findings [11]. Their routes, species, durations, and mechanistic assays differ; they neither confirm a pathway here nor explain cross-tissue staining differences.

Lower calcium is compatible with altered intestinal transport [5] and calcium-regulatory processes [2]. Researchers have investigated parathyroid calcium-sensing changes in chronic-renal-failure rats [22], a different setting. Lower iron is compatible with aluminum–iron binding/transport interactions [4], experimental hematopoietic alterations [23], changes in

serum iron-associated proteins [24], and erythroid abnormalities after long-term ingestion [25]. Splenic hemosiderosis is relevant to iron handling but does not prove hemolysis. Without parathyroid hormone, vitamin D, ferritin, transferrin saturation, or erythrocyte indices, the study cannot resolve the dominant mineral-regulatory mechanisms.

Quantitative immunohistochemistry was restricted to four organs in high-dose and control males at day 90. Histology was qualitative, without animal-level severity distributions. The study did not measure caspase-3 activity directly, include complementary apoptosis assays, or measure aluminum at the organ level. These scope limits do not change the observed associations but limit dose–time, sex-specific, and mechanistic inferences.

Conclusion

Chronic oral aluminum chloride exposure was associated with increased caspase-3 immunoreactivity, renal, hepatic, and splenic histopathological abnormalities, and reduced serum calcium and iron in male rats. These findings characterize caspase-3 protein immunoreactivity and associated injury, but do not confirm enzymatic activation or apoptosis. Day-90 high-dose–control comparisons do not establish an organ susceptibility ranking.

Ethical Approval

Not applicable.

Acknowledgment

The authors thank the animal-house and histopathology staff at Al-Qasim Green University for technical assistance and the National Center for Drug Control and Research, Baghdad, for providing animals.

Funding

No external funding supported this research.

Conflicts of Interest

The authors report no competing interests.

References

[1] Igbokwe IO, Igwenagu E, Igbokwe NA. Aluminium toxicosis: a review of toxic actions and effects. Interdiscip Toxicol. 2019;12(2):45-70. [DOI: 10.2478/intox-2019-0007]

Klein GL. Aluminum toxicity to bone: a multisystem effect? Osteoporos Sarcopenia. 2019;5(1):2-5. [DOI: 10.1016/j.afos.2019.01.001]

[3] Teschke R. Aluminum, arsenic, beryllium, cadmium, chromium, cobalt, copper, iron, lead, mercury, molybdenum, nickel, platinum, thallium, titanium, vanadium, and zinc: molecular aspects in experimental liver injury. Int J Mol Sci. 2022;23(20):12213. [DOI: 10.3390/ijms232012213]

[4] Ward RJ, Zhang Y, Crichton RR. Aluminium toxicity and iron homeostasis. J Inorg Biochem. 2001;87(1-2):9-14. [DOI: 10.1016/S0162-0134(01)00308-7]

[5] Orihuela D. Inhibitory effect of aluminium on calcium absorption in small intestine of rats with different thyroid hormone status. J Inorg Biochem. 2009;103(11):1542-7. [DOI: 10.1016/j.jinorgbio.2009.07.017]

[6] Patergnani S, Danese A, Bouhamida E, Aguiari G, Previati M, Pinton P, et al. Various aspects of calcium signaling in the regulation of apoptosis, autophagy, cell proliferation, and cancer. Int J Mol Sci. 2020;21(21):8323. [DOI: 10.3390/ijms21218323]

[7] D'Arcy MS. Cell death: a review of the major forms of apoptosis, necrosis and autophagy. Cell Biol Int. 2019;43(6):582-92. [DOI: 10.1002/cbin.11137]

[8] McIlwain DR, Berger T, Mak TW. Caspase functions in cell death and disease. Cold Spring Harb Perspect Biol. 2013;5(4):a008656. [DOI: 10.1101/cshperspect.a008656]

[9] Li M, Song M, Ren LM, Xiu CY, Liu JY, Zhu YZ, et al. AlCl3 induces lymphocyte apoptosis in rats through the mitochondria-caspase dependent pathway. Environ Toxicol. 2016;31(4):385-94. [DOI: 10.1002/tox.22051]

[10] Zhang H, Wei M, Lu X, Sun Q, Wang C, Zhang J, et al. Aluminum trichloride caused hippocampal neural cells death and subsequent depression-like behavior in rats via the activation of IL-1β/JNK signaling pathway. Sci Total Environ. 2020;715:136942. [DOI: 10.1016/j.scitotenv.2020.136942]

[11] Othman MS, Fareid MA, Abdel Hameed RS,

Abdel Moneim AE. The protective effects of melatonin on aluminum-induced hepatotoxicity and nephrotoxicity in rats. Oxid Med Cell Longev. 2020;2020:7375136. [DOI: 10.1155/2020/7375136]. Erratum in: Oxid Med Cell Longev. 2026;2026:9784046. [DOI: 10.1155/omcl/9784046]

[12] Murad HM, Neamah GAK, Shareef HK, AL-Mussawy AN. Time- and dose-dependent neurotoxicity of aluminum chloride: oxidative stress, cholinergic dysfunction, and histopathological alterations in male rat brain. Int J Med Toxicol Forensic Med. 2026;16:E53006. [DOI: 10.22037/ijmtfm.v16.53006]

[13] Percie du Sert N, Hurst V, Ahluwalia A, Alam S, Avey MT, Baker M, et al. The ARRIVE guidelines 2.0: updated guidelines for reporting animal research. PLoS Biol. 2020;18(7):e3000410. [DOI: 10.1371/journal.pbio.3000410]

[14] Kumar A, Prakash A, Dogra S. Neuroprotective effect of carvedilol against aluminium induced toxicity: possible behavioral and biochemical alterations in rats. Pharmacol Rep. 2011;63(4):915-23. [DOI: 10.1016/S1734-1140(11)70607-7]

[15] Suvarna KS, Layton C, Bancroft JD, editors. Bancroft's theory and practice of histological techniques. 8th ed. Amsterdam: Elsevier; 2019. [Link]

[16] Holm S. A simple sequentially rejective multiple test procedure. Scand J Stat. 1979;6(2):65-70. [Link]

[17] Mesole SB, Alfred OO, Yusuf UA, Lukubi L, Ndhlovu D. Apoptotic inducement of neuronal cells by aluminium chloride and the neuroprotective effect of eugenol in Wistar rats. Oxid Med Cell Longev. 2020;2020:8425643. [DOI: 10.1155/2020/8425643]

[18] Khalaf AEA, Morgan AM, Mekawy MM, Ali MF. Immunotoxicity following pre- and post-natal aluminum exposure in rats. Toxicol Res. 2008;24(1):51-8. [DOI: 10.5487/TR.2008.24.1.051]

[19] Yu H, Zhang J, Ji Q, Yu K, Wang P, Song M, et al. Melatonin alleviates aluminium chloride-induced immunotoxicity by inhibiting oxidative stress and apoptosis associated with the activation of Nrf2 signaling pathway. Ecotoxicol Environ Saf. 2019;173:131-41. [DOI: 10.1016/j.ecoenv.2019.01.095]

[20] Liu P, Guo C, Cui Y, Zhang X, Xiao B, Liu M, et al. Activation of PINK1/Parkin-mediated mitophagy protects against apoptosis in kidney damage caused by aluminum. J Inorg Biochem. 2022;230:111765. [DOI: 10.1016/j.jinorgbio.2022.111765]

[21] Wei H, Li D, Luo Y, Wang Y, Lin E, Wei X. Aluminum exposure induces nephrotoxicity via fibrosis and apoptosis through the TGF-β1/Smads pathway in vivo and in vitro. Ecotoxicol Environ Saf. 2023;249:114422. [DOI: 10.1016/j.ecoenv.2022.114422]

[22] González-Suárez I, Naves M, Díaz-Corte C, Fernández-Martín JL, Menéndez-Rodríguez P, Cannata-Andía JB. Effect of aluminium on calcium-sensing receptor expression, proliferation, and apoptosis of parathyroid glands from rats with chronic renal failure. Kidney Int Suppl. 2003;(85):S39-43. [DOI: 10.1046/j.1523-1755.63.s85.10.x]

[23] Chmielnicka J, Nasiadek M, Lewandowska-Żyndul E, Pińkowski R. Effect of aluminum on hematopoiesis after intraperitoneal exposure in rats. Ecotoxicol Environ Saf. 1996;33(3):201-6. [DOI: 10.1006/eesa.1996.0026]

[24] Zhang L, Li X, Gu Q, Zhu Y, Zhao H, Li Y, et al. Effects of subchronic aluminum exposure on serum concentrations of iron and iron-associated proteins in rats. Biol Trace Elem Res. 2011;141(1-3):246-53. [DOI: 10.1007/s12011-010-8725-y]

[25] Vittori D, Nesse A, Pérez G, Garbossa G. Morphologic and functional alterations of erythroid cells induced by long-term ingestion of aluminium. J Inorg Biochem. 1999;76(2):113-20. [DOI: 10.1016/S0162-0134(99)00122-1]